LOCALLY REGULARIZED SNAKES THROUGH SMOOTHING B-SPLINE FILTERING

Jérôme Velut, Hugues Benoit-Cattin, and Christophe Odet

CREATIS, CNRS UMR 5515, Inserm U 630
INSA, Bât. B. Pascal, 69621 Villeurbanne, France
email: jerome.velut@creatis.insa-lyon.fr
web: www.creatis.insa-lyon.fr

ABSTRACT

In this paper we propose a locally regularized snake based on smoothing-spline filtering. The proposed algorithm associates this regularization process to a force equilibrium scheme leading the snake's deformation. The regularization level is controlled through a unique parameter that can vary along the contour: It provides a locally regularized smoothing B-snake that offers a powerful framework to introduce prior knowledge. We illustrate the snake behavior on MRI images, with global and local regularization.

1.   INTRODUCTION

Active contour models (or snakes) are well-adapted for edge detection and segmentation. Since snakes were introduced by Kass et al.[1], they have been widely used in many domains and improved using different contour representations and deformation algorithms. Menet et al. proposed the B-snakes in [2] that take advantages of the B-spline representation: a local control of the curve continuity and a limited number of processed points increase the convergence speed and the reliability of the segmentation. At the same time, Cohen et al. [3] focused on external forces that drive the snake toward the features of interest in the image and proposed the balloon force, that increases considerably the attainability zone. Then, Xu et al. [4] defined another external force called GVF that bring a better control on the deformation directions. Beside these works, the multi-resolution frameworks have been integrated within the active contours: Wang et al. [5] used a B-spline representation that allows a coarse-to-fine evolution of the snake. Brigger et al. [6, 7] extended Wang's technique with a multi-scale approach in both the image and parametric contour domain. Finally, Precioso et al. [8] proposed a region-based active contour that achieves the real-time computation adapted to video segmentation. They extended their model by applying a smoothing B-spline filter [9, 10] on the contour. It increases considerably the robustness to noise without additional computation. Recently, new energies have been proposed by Jacob et al. [11] who unify the edge-based with the region-based scheme.

Existing snakes suffer several limitations when a local regularization is wanted: with the original snake [1], a local regularization involves a matrix inversion step at each iteration. Although B-snakes [6] avoid this by implicitizing the internal energy, the proposed solution induced a varying sampling step when we need to regularize locally the snake. Consequently, prior knowledge will be difficult to integrate in the contour sampling step. The smoothing B-spline filtering method of [8] doesn't deal with local regularization and has a strong initialization-dependent minimization process linked to the regularization algorithm proposed.

In this paper, we propose to regularize locally a snake while keeping a uniform sampling step. The presented approach is based on smoothing-spline filtering that is controlled through a unique parameter λ. The next section reminds the snake concepts and their interaction with B-splines. Section 3 details the proposed algorithm named LRSB-snake that stands for Locally Regularized Smoothing B-snake. Section 4 presents experiments' results on real and synthetic images.

2.   SNAKES AND B-SPLINES

2.1   Snake basics.

A snake [1] is a parametric curve $g(s)=(x(s),y(s))$ that evolves on an image $I(x,y)$ and stops on the features of interest. The snake evolution is controlled by an energy minimization. The curve has to go where its total energy E_{snake}, defined in equation (1), is minimal.

$$E_{snake} = \int_s E_{int}(g(s)) + E_{ext}(g(s))ds \qquad (1)$$

where E_{int} has a regularization role and is the internal energy that traduces shape constraints on the curve; Where E_{ext} is the external energy that drives the snake toward image features.

Typically, E_{ext} is computed from the gradient of the image (Eq. 2) as the usual goal of a snake is to detect object boundaries.

$$E_{ext} = -\left|\nabla I(x,y)\right|^2 \qquad (2)$$

The variational method used in [1] to complete the minimization of equation (1) leads to a force balance given by:

$$A \cdot g(k) + f(k) = 0 \qquad (3)$$

where *A* is a pentadiagonal banded matrix built from E_{int}, where $g(k)=(x(k),y(k))$ is the discrete version of the $g(s)$ curve and where $f(k)=(f_x(k),f_y(k))$ constitutes the external forces computed at each *k* snake's point as follows:

$$f(k) = (f_x(k), f_y(k)) = \left(\frac{\partial E_{ext}}{\partial x(k)}, \frac{\partial E_{ext}}{\partial y(k)} \right) \quad (4)$$
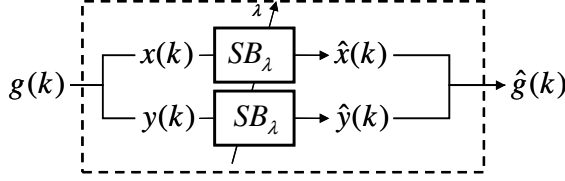

Figure 1. Smoothing B-spline filtering of a parametric discrete signal g(k).

The gradient descent method determines (Eq. 5) the new positions of the snake points $(g_i(k))$ at each iteration.

$$g_i(k) = (A + \gamma \cdot I)^{-1} (\gamma \cdot g_{i-1}(k) - f(k)) \quad (5)$$

where γ is a step-size parameter and *i* is the iteration index of the gradient descent evolution.

This method is used by Menet et al. [2] where $g(s)$ is represented through B-spline. Such model offers a better local continuity control and a faster convergence. In [6], Brigger et al. show that the B-spline representation of a snake induces an built-in smoothness of the curve. They also propose a variant sample step of the curve to bring an implicit regularization. The internal energy and its regularization effect are implicit and the iterative process enounced in equation (5) is simplified to:

$$g_i(k) = g_{i-1}(k) - \gamma \cdot f(k) \quad (6)$$

f(k) may be balloon forces [12], or gradient vector flow [4] or any other forces that lead the snake to the desired features.

2.2 Regularization through Smoothing B-spline filtering

Although variant sample step enables regularization, the lack of information under the snake at low resolution may make difficult the incorporation of prior knowledge in an initial model. Precioso et al. [8] propose the use of a low-pass IIR filter on each parametric components of the curve to regularize the snake. This filter is the smoothing B-spline filter described in [10]. It computes a more or less smooth approximation $\hat{g}(k)$ of a finite set of points $g(k)$, where the continuous representation $\hat{g}(s)$ of $\hat{g}(k)$ minimizes the following functional:

$$\varepsilon_s^2 = \sum_{k=-\infty}^{+\infty} \left(g(k) - \hat{g}(k) \right)^2 + \lambda \int_{-\infty}^{+\infty} \left(\frac{\partial^2 \hat{g}(s)}{\partial s^2} \right)^2 ds \quad (7)$$

where λ is the parameter that tunes the smoothness constraint of $\hat{g}(k)$.

Figure 1 shows the filtering process involved in [8]. It is based on the filtering of a parametric signal by the SB_λ filter which cut-off frequency is controlled by λ (Figure 2).

Nevertheless, the way of using the smoothing B-spline filter in the Precioso's algorithm has some drawbacks. In-

deed, the regularization amount increases as the iterations and consequently the final snake smoothness is dependent on the initial one. Precioso et al. [8] gives empiric values of suitable λ in their algorithm (λ can take value in [0.1,1]) to avoid these problems.
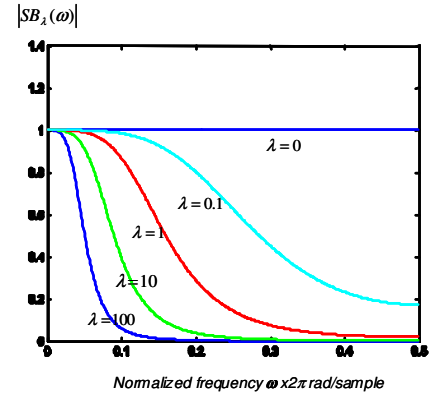

Figure 2: Frequency response of the smoothing-spline filter SB_λ for different values of λ.

We propose in the next section another algorithm that regularizes a snake with a smoothing B-spline filter, without the drawbacks mentioned above and without any λ restriction. In this algorithm, the regularization may be either global or local.

3. LOCALLY REGULARIZED SMOOTHING BSNAKE

An overview of the proposed LRSB-snake is given Figure 3. From an initial contour $\hat{g}_0(k)$ and the image to segment, we compute the deformation forces (see §3.1). The regularization is done by smoothing the deformation forces. We can apply a global regularization (§3.2) or a local one (§3.3). The contour is then moved by applying the regularized deformation forces. To enforce a similar behavior of the smoothing process at each iteration, the contour may be resampled. If the contour is stabilized, the iterative process is stopped.

3.1 Deformation force computation

The external forces are directly derived from the image to segment. They guide the snake to the desired features. Within our LRSB-snake algorithm any type of external forces may be used, such as Xu et al. Gradient Vector Flow [4] that computes a diffusion of the image gradient or Cohen et al. balloon forces [12] that simulates a pressure force and makes the snake swelled. The sum of every considered forces gives the deformation vector $d_i(k)$ at each point *k* and at each iteration *i*. Without doing any regularization (i.e. $\lambda=0$), we obtain a deformation equation (Eq. 8) that minimizes the external energy represented by the image forces. Note that this deformation equation is similar to the one of [8] (region-based deformation).

$$\hat{g}_{i+1}(k) = g_{i+1}(k) \begin{cases} = \hat{g}_i(k) + \gamma \cdot \hat{d}_i(k) \\ = g_i(k) + \gamma \cdot d_i(k) \end{cases} \quad (8)$$
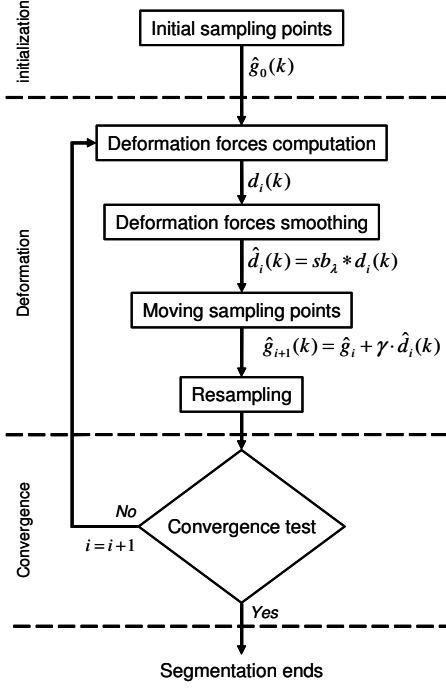
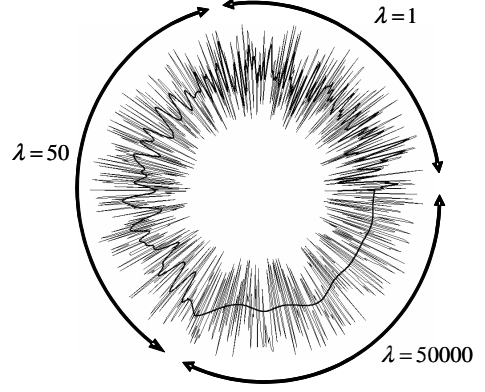Figure 3: Flow-chart of the locally regularized smoothing B-snake algorithm.

Figure 4. Spatially-variant smoothing-spline filtering. The input signal is the thin noisy circle. This signal is filtered through a smoothing-spline filter where the smoothing parameter λ varies along the contour. The resulting signal is represented in bold

where i is the iteration index, $g(k)$ are the snake points, $d_i(k)$ are the deformation vectors i.e the external forces and γ is the step-size involved in the variational method of the original snake.

This equation is similar to the original snake's one (Eq.5) with:

$$d(k) = (d_x(k), d_y(k)) = (f_x(k), f_y(k)) \qquad (9)$$

where f is defined in (Eq.4).

3.2 Global regularization process through deformation force smoothing

Regularization of the deformable model is essential to ensure a good robustness to noise of such segmentation approach. As in [8], we choose to constrain the curvature of the contour with a smoothing B-spline filter that minimizes the curvature optimally [9] according to a single parameter λ.

Equation (10) gives the snake regularized by the SB_λ approximation filter at iteration i.

$$\hat{g}_i(k) = sb_\lambda(k) * g_i(k) \qquad (10)$$

From equations (8) and (10), we obtain equation (11) that yields the deformation and motion steps of the algorithm (Figure 3).

$$\hat{g}_{i+1}(k) = \hat{g}_i(k) + (\gamma \cdot d_i(k)) * sb_\lambda(k) \qquad (11)$$

Finally, from equation (11) and using the Z transform, we obtain:

$$\hat{G}_{i+1}(z) = \hat{G}_0(z) + \gamma \cdot \sum_{j=0}^{i} D_j(z) \cdot SB_\lambda(z) \qquad (12)$$

It is clear in equation (11) that we realize the snake regularization by a smoothing filtering of the deformation forces (Figure 3). Consequently (Eq. 12), an infinite iterative process does not lead to an infinite successive convolution of d_i. Compared to [8], the regularization does not depend on the number of iterations. It allows λ to control the cut-off frequency of the SB_λ approximation filter -and thus the regularization level- by taking any real positive value. As the regularization is done by a digital filtering, it preserves the processing speed mentioned in [8].

Note that a 1-D filter is usually applied on a uniformly sampled signal. As we want to keep the same filter frequency response which is λ-dependent, we enforce a uniform sampling of the contour in our algorithm.

3.3 Local regularization process

In our regularization process, λ value is not constraint to be globally set. Consequently, λ can differ from node to node in order to provide a local regularization. From the regularization term of equation (11), one can write the following equation:

$$\hat{D}_i(z) = SB_\lambda(z) \cdot D_i(z) \qquad (13)$$

Where

$$SB_\lambda(z) = \frac{z + 4 + z^{-1}}{a + b \cdot (z + z^{-1}) + c \cdot (z^2 + z^{-2})} \qquad (14)$$

with $a = 4 + 36 \cdot \lambda$, $b = 1 - 24 \cdot \lambda$ and $c = 6 \cdot \lambda$.

It appears in equation (14) that the filter coefficients a, b and c are λ-dependent. We propose to make SB_λ space-varying by making λ dependent on k, the contour point number. Thus, a, b and c become

$$a_k = 4 + 36 \cdot \lambda_k, \ b_k = 1 - 24 \cdot \lambda_k, \ c_k = 6 \cdot \lambda_k \qquad (15)$$

and equation (14) becomes:

$$SB_\lambda(z) = \frac{z + 4 + z^{-1}}{a_k + b_k \cdot (z + z^{-1}) + c_k \cdot (z^2 + z^{-2})} \qquad (16)$$
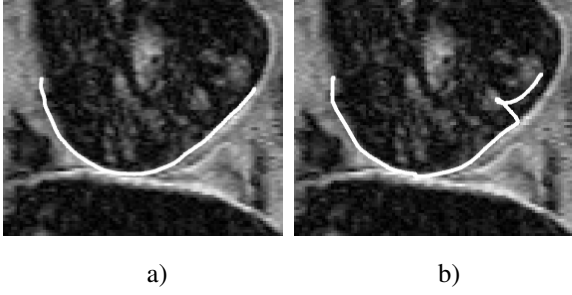
Figure 5: MRI image of a guinea-pig knee and an initial 67-points snake. Segmentation results with a) $\lambda = 1000$, 630 iterations and b) $\lambda=71$, 1280 iterations.

Consequently, each node of the snake has its own regularization rate. We are able to affect different values of λ along the contour (Figure 4) according to local image information or prior knowledge introduced in the initial model.

4. RESULTS

This section gives results obtained with the proposed LRSB-snake algorithm. First the global regularization mode is illustrated on MRI images. Then, the LRSB-snake is applied on an angio-MRI image to illustrate the advantage of a local regularization. All these results have been obtained with the following external forces: Laplacian vectors of a Gaussian-blurred version of the image combined with a balloon force to increase the convergence speed.

4.1 Global regularization

Figure 5-a shows an MR image of a guinea pig knee and an initial smoothing B-snake. The feature to detect is the femoral border. With a too low λ value (λ=71), the final result obtained after 1280 iterations is corrupted by a local minimum (Figure 5-b). We set a larger λ value (λ=1000) to avoid this artifact (Figure 5-c). The final result obtained after 630 iterations is close to the wanted femoral border.

4.2 Local regularization

Figure 6 shows the drawbacks of a globally-set regularization. This deformed circle comprises 3 parts, each having a different amount of local curvature. With a low global λ (Figure 6-a), the snake is not able to find any true boundaries. With a high global λ, an approximated boundary of the object is found (Figure 6-b). But if the different part are known, an adapted local λ gives to the snake a good behaviour and each part are well segmented.

Figure 7 illustrates the behavior of the LRSB-snake on a angio-MRI. On Figure 7-a, a high regularization rate does not allow the snake to outline the true boundary. Figure 7-b shows the result with a small value, where the balloon forces induce a leak of the snake. The LRSB-Snake is then applied on this image (Figure 7-c). A λ map gives the λ values at each image position. In this example, the λ map is

manually defined, with values empirically determined as follows. Positions where the contour is well visible take a small λ value (λ=1), and positions where the contour tends to disappear take with a high λ value (λ=300). One can observe on Figure 7-d that such a local regularization prevents the leak, manages correctly the ghost gradient and stops the swell at the top.
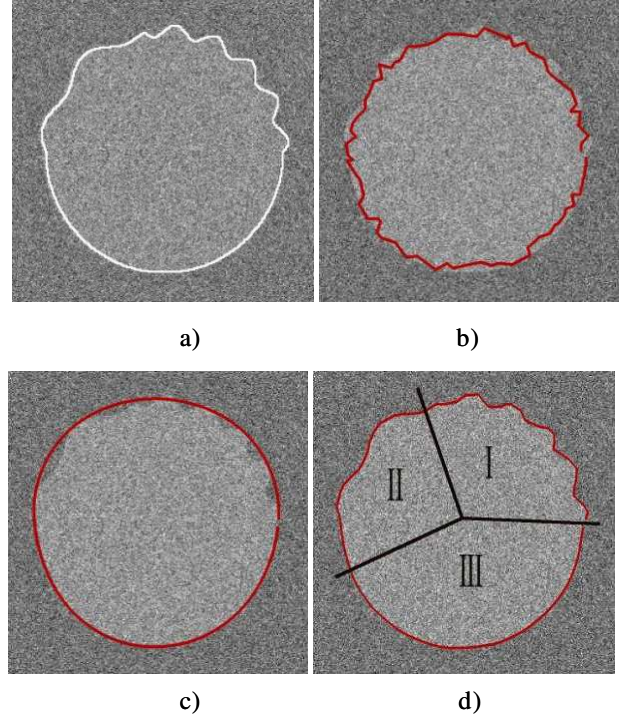

Figure 6: Constant and locally regularized 100-points smoothing B-snake on a synthesis image. a) Noisy object with the reference contour in white. b) Final segmentation with global low λ (λ=1). Local minima are too attractive. c) Global high λ (λ=100). The object is localized but not precisely outlined. d) Locally regularized smoothing b-snake. I: $\lambda = 1$. II: $\lambda = 10$, III: $\lambda = 100$.

5. CONCLUSIONS

In this paper, we propose a Locally Regularized Smoothing B-snake algorithm. The regularization process uses an approximating smoothing-spline filter applied directly on the snake node displacement. This algorithm conserves the advantages of snake algorithms and offers a local control of the regularization through the λ value defined at each snake nodes. As the regularization is implemented through a recursive implementation of a digital filter, this algorithm is fast.

This algorithm associated to pertinent local λ definition offers a powerful tool for introducing prior knowledge and consequently makes the segmentation process more robust.
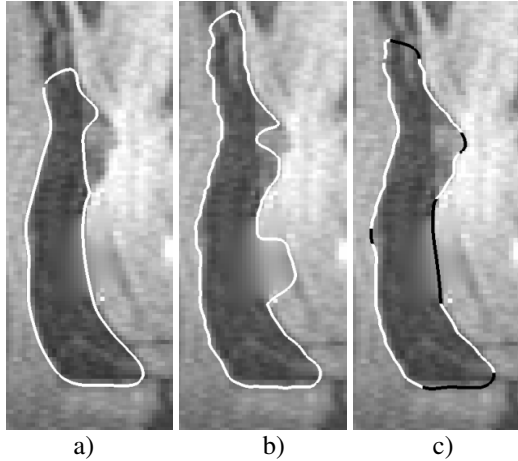
| a) | b) | c) |

Figure 7: a) Final segmentation using λ=300, 250 iterations. b) Final segmentation using λ=1, 310 iterations. c) Final segmentation using local λ values (black for λ=300, white for λ=1), 330 iterations.

6. ACKNOWLEDGEMENT

7. REFERENCE

[1] M. Kass, A. Witkin, and D. Terzopoulos, "Snakes: Active Contour Models," presented at Proceedings - First International Conference on Computer Vision., London, Engl, 1987.

[2] S. Menet, P. Saint-Marc, and G. Medioni, "B-Snakes : Implementation and Application to Stereo," *Image Understanding Workshop.*, pp. 720-726, 1990.

[3] L. D. Cohen and I. Cohen, "Finite-element methods for active contour models and balloons for 2-D and 3-D images," *IEEE Transactions on Pattern Analysis and Machine Intelligence*, vol. 15, pp. 1131-1147, 1993.

[4] C. Xu and J. L. Prince, "Generalized gradient vector flow external forces for active contours," *Elsevier - Signal Processing.*, vol. 71, pp. 131-139, 1998.

[5] M. Wang, J. Evans, L. Hassebrook, and C. Knapp, "A Mutlistage, Optimal Active Contour Model," *Transactions on Image Processing*, vol. 5, pp. 1586-1591, 1996.

[6] P. Brigger, J. Hoeg, and M. Unser, "B-spline snakes: a flexible tool for parametric contour detection," *IEEE Transactions on Image Processing*, vol. 9, pp. 1484-1496, 2000.

[7] P. Brigger and M. Unser, "Multi-scale B-spline snakes for general contour detection," presented at Wavelet Applications in Signal and Image Processing VI, Jul 22-23 1998, San Diego, CA, United States, 1998.

[8] F. Precioso, M. Barlaud, T. Blu, and M. Unser, "Robust Real-time Segmentation of Images and Videos Using a Smoothing-spline Snake-Based algorithm.," *Transactions on Image Processing*, vol. In Press, 2005.

[9] C. H. Reinsch, "Smoothing by Spline Functions," *Numerisch Mathematik*, vol. 10, pp. 177-183, 1967.

[10] M. Unser, A. Aldroubi, and M. Eden, "B-spline signal processing. Part I. Theory," *IEEE Transactions on Signal Processing*, vol. 41, pp. 821-833, 1993.

[11] M. Jacob, T. Blu, and M. Unser, "Efficient energies and algorithms for parametric snakes," *IEEE Transactions on Image Processing*, vol. 13, pp. 1231-1244, 2004.

[12] L. D. Cohen, "On Active Contour Models," INRIA, Rocquencourt, Programmation, Calcul Symbolique et Intelligence Artificielle 1075, 1989.